View metadata, citation and similar papers at core.ac.uk
brought to you by CORE
provided by Repositorio Academico Digital UANL

doi: 10.4149/gpb_2017011

Biodegradable nanoparticles loaded with tetrameric melittin: preparation and membrane disruption evaluation

Azucena Gonzalez-Horta[1*], Arely Matamoros-Acosta[1*], Abelardo Chavez-Montes[2], Rocio Castro-Rios[3] and Jorge Lara-Arias[4]

[1] *Laboratory of Genomic Science, Faculty of Biological Sciences, Universidad Autonoma de Nuevo Leon, 66455 San Nicolas de los Garza, N.L. Mexico*
[2] *Department of Chemistry, Faculty of Biological Sciences, Universidad Autonoma de Nuevo Leon, 66455 San Nicolas de los Garza, N.L. Mexico*
[3] *Department of Analytical Chemistry, Faculty of Medicine, Universidad Autonoma de Nuevo Leon, 66544 San Nicolas de los Garza, N.L. Mexico*
[4] *Bone and Tissue Bank, University Hospital Dr. Jose E. Gonzalez, Monterrey, Mexico*

Abstract. Melittin is the main component of bee venom consisting of 26 amino acids that has multiple effects, including antibacterial, antiviral and anti-inflammatory in various cell types. This peptide forms pores in biological membranes and triggers cell death. Therefore it has potential as an anti-cancer therapy. However, the therapeutic application of melittin is limited due to its main side effect, hemolysis, which is especially pronounced following intravenous administration. In the present study, we formulated tetrameric melittin-carrying poly-D,L-lactic-co-glycolic acid nanoparticles (PLGA-NPs) and analyzed the lytic activity of this system on liposomes that resembles breast cancer cells. Tetrameric melittin binds avidly to PLGA-NPs with an encapsulation efficiency of 97% and retains its lytic activity demonstrating the effectiveness of PLGA-NPs as nanocarriers for this cytolytic peptide.

Key words: Melittin — PLGA nanoparticles — Liposomes — Leakage — Fluorescence — Circular dichroism

Introduction

Melittin is a naturally occurring cationic antimicrobial peptide obtained from the toxic component in the venom of the European honey bee, *Apis mellifera* (Habermann 1977). It is a small linear peptide composed of 26 amino acids having the sequence NH_2-GIGAVLKVLTTGLPALISWIKRKRQQ-$CONH_2$. The amino-terminal region (residues 1–20) of this peptide is predominantly hydrophobic whereas the carboxy-terminal region (residues 21–26) is hydrophilic due to the presence of a stretch of positively charged amino acids (Raghuraman and Chattopadhyay 2004a). Due to this amphiphilic property of melittin it becomes water-soluble and spontaneously associates with natural and artificial membranes (Raghuraman and Chattopadhyay 2004b). Because of poor cell selectivity, it exhibits strong lytic activity against both bacterial and mammalian cells (Raghuraman and Chattopadhyay 2007). Melittin is intrinsically fluorescent due to the presence of a single tryptophan residue at the 19th position. The presence of this tryptophan is utilized as the probe to study the interaction of the peptide with membranes and membrane-mimetic systems (Pott et al. 2001). Melittin's action was thought to involve membrane pore formation or membrane perturbation, resulting in the disruption of the membrane (Allende et al. 2005; Yang et al. 2001; Shigeri et al. 2016). This peptide is an attractive anticancer candidate because of its wide-spectrum lytic properties. Although cytotoxic to a broad spectrum of tumor cells (Liu et al. 2008; Gajski et al. 2011; Jeong et al. 2014) melittin is also toxic to red blood cells and its therapeutic potential cannot be achieved without a proper delivery vehicle. This could be overcome by melittin nanoparticles that possess the ability

Correspondence to: Azucena Gonzalez-Horta, Laboratory of Genomic Science, Faculty of Biological Science, Universidad Autonoma de Nuevo Leon, 66455 Monterrey, N.L. Mexico
E-mail: azucena.gonzalezhr@uanl.edu.mx
* These authors have contributed equally to this paper

to safely deliver a significant amount of melittin and to target and kill cancer cells. In recent years, nanoparticles (NPs) were prepared from biodegradable polymers such as poly-D,L-lactic-co-glycolic acid (PLGA), a copolymer of lactic and glycolic acid approved by FDA for certain clinical uses. The polymer degradation time can vary from several months to years, depending on the molecular weight and copolymer ratio. PLGA is nontoxic, nonirritating and fully biodegradable with good biocompatibility and human adaptability. *In vivo*, the final degradation product of PLGA is lactate that can be metabolized by intravital cells (Pan et al. 2011). Also, the physicochemical properties of bee venom-loaded PLGA-NPs has been characterized in order to design and optimize a suitable sustained release system (Bala et al. 2004), however, the melittin lytic activity on unilamellar lipid bilayer (liposomes) once incorporated into nanoparticles has not been evaluated. Liposomes are synthetic mimics of cellular membranes and represent an experimental system widely used for more than 30 years in the field of biochemical research involving lipids. Another promising solution to reduce melittin´s cytotoxicity is to introduce cell selectivity by modulating melittin assembly and its inherent secondary structure in the aqueous environment of the bloodstream (Park et al. 2015). In this study, we have performed spectroscopic studies aimed at disclosing the basic structural characteristics of tetrameric melittin after been incorporated into PLGA nanoparticles (PLGA-NPs).

Materials and Methods

Materials

Melittin (research grade) was purchased from Sigma Aldrich chemicals (Saint Louis, MO). The lipids L-a-phosphatidylcholine from egg yolk (PC), 1,2-diacyl-*sn*-glycero-3-phosphatidylethanolamine (PE), L-a-phosphatidic acid sodium salt (PA) and 1,2-diacyl-*sn*-glycero-3-phospho-L-serine (PS) were from Avanti polar lipids (Alabaster, AL). PLGA (MW 50,000–75,000: lactide-co-glycolide ratio 85:15) was from Sigma Aldrich (Saint Louis, MO). ANTS (8-aminonaphthalene-1,3,6-trisulphonic acid) and DPX (N,N'-p-xylene-bis-pyrimidinium bromide) were from Sigma Aldrich (Saint Louis, MO).

Methods

Melittin preparation

One milligram of melittin was dissolved in 1 ml buffer Hepes 20 mM pH 7.4 at 25°C to maintain the monomeric conformation. The tetrameric melittin conformation was obtained preparing peptide stock solution (final concentration 1.8 mM) in buffer 20 mM Hepes, 250 mM NaCl (pH 7.4). To monitoring the a-helical content of melittin in solution under each experimental conditions, far-UV circular dichroism was recorder.

Nanoparticles preparation

Nanoparticles were prepared by double emulsion solvent evaporation method using power ultrasound. Double emulsion was prepared by two-step emulsification process. In the first step, in order to make the primary emulsion (W1/O), 20 mg poly(lactic-co-glycolic acid) (PLGA, m.w. 17,000) were dissolved in 1.5 ml of ethyl acetate and 20 mg of Lutrol F 68 (Poloxamer 188, BASF) properly to form a clear solution. This mixture was homogenized properly using ultrasonic homogenizer for 90 s (Branson Ultrasonics Corp, Danbury, CT, USA). In the second step, the primary emulsion (W1/O) was dispersed in the outer aqueous phase (W2) containing magnesium chloride 3.0 % w/w. This mixture was homogenized *via* ultrasonic homogenizers for 90 s which produced double emulsion (W1/O/W2). Afterword, the organic solvent evaporation from dispersed droplets via rotary evaporator (Heidolph instruments GmbH and Co. Alemania) has led to solidified PLGA-NPs. Then 40 µl of an aqueous solution of tetrameric melittin (1.8 mM) was added to the preformed nanoparticles and the residual free (unbound) melittin washed out by centrifugation at 35,000 rpm for 3 hours.

Hydrodynamic size measurement

The mean diameter and polydispersity index (PDI) of the nanoparticles were measured by dynamic light scattering (DLS) using a ZS90 (Malvern Instruments, R.U.) working at an angle of 90°. The analysis was performed right after the preparation of the nanoparticle dispersions. Before analysis, the samples were diluted 50 times in Milli-Q water to reach a level of light scattering signal recommended by the supplier of the light scattering apparatus. Each sample was analyzed in triplicate.

Determination of melittin assembled in nanoparticles

Samples of nanoparticles loaded with melittin were analyzed by measuring the fluorescence intensity emitted by tryptophan 19 (excitation, 280 nm; emission, 351 nm) and interpolating the value on a calibration curve prepared for this purpose ($y = 49.036x + 1.17$; $R^2 = 0.9882$). The calibration curve was obtained measuring the emission of melittin in buffer Hepes 20 mM (pH 7.4). The amount of melittin incorporated in nanoparticle was also confirmed by Bradford assay for which, the melittin-nanoparticles suspension were centrifuge at 10,000 rpm for 30 min to remove the unbound

melittin. The melittin in the supernatant was quantified as recommended by the manufacturer (Bio-Rad Protein Assay).

Circular dichroism

Conformational changes occurring once the peptide was assembled into nanoparticles were monitored by circular dichroism (CD) spectroscopy. CD spectra were registered in a J-1100 spectropolarimeter (JASCO, Easton, MD) equipped with a Koolance Peltier-type holder for temperature control at 25°C. All spectra were recorded in 0.2 nm wavelength increments with a 4 s response and a bandwidth of 1 nm. The secondary structure of the assembled and native melittin was assessed from spectra registered over the 190–240 nm (far-UV) at a scan rate of 50 nm/min. Each spectrum is the average of 5 scans with a full scale sensitivity of 50 mdeg. All spectra were corrected for background by subtraction of appropriate blanks and were smoothed making sure that the overall shape of the spectrum remains unaltered. Measurements were made in a 0.1 cm cuvette with melittin solutions (70 mM) or a diluted suspension of nanoparticles containing 100 mg of peptide *per* milliliter. The samples were equilibrated in buffer Hepes 5 mM pH 7.4. Helix content of peptides was assumed to be directly proportional to mean residue ellipticity (MRE) at 222 nm, $[\theta]_{222}$. One hundred percent helicity was calculated using the formula $^{max}[\theta]_{222} = -40{,}000 \times [(1 - 2.5/h)] + (100 \times T)$, where h is number of amino acid residues and T is temperature in °C (Scholtz et al. 1991; Jamasbi et al. 2014). Percentage helicity was then calculated as $100 \times [\theta]_{222} / {}^{max}[\theta]_{222}$.

Intrinsic fluorescence

The polarity of the microenvironment around tryptophan residue at position 19th was investigated by measuring the intrinsic fluorescence of melittin in buffer and melittin-PLGA-NP after sample excitation with 280 nm UV radiation. Emission spectra were registered from 300 to 500 nm in a LS45 spectrofluorometer (Perkin-Elmer Inc.) with 1 cm cells. Nanoparticle and melittin samples were prepared in buffer 20 mM Hepes, 150 mM NaCl (pH 7.4) and the protein concentration was adjusted to 15 μg/ml.

Vesicle preparation

We used the mixture PC/PE/PS (50:40:10 w/w) to simulate membranes healthy mammary epithelial cells and the mixture PC/PE/PS/PA (50:25:15:10 w/w) to resemble the membranes of breast cancer cells. As representative compounds of erythrocyte membrane we used PC liposomes. The lipids were mixed in chloroform/methanol 2:1 (v/v) and the mixture was dried under a N_2 stream and then for 2 h in a vacuum chamber to form a thin film which was later resuspended by addition of 1 ml of 50 mM Hepes buffer (pH 7.4), containing 150 mM NaCl and incubated for 2 h with eventual vortexing at 25°C for each lipid mixture. Large unilamellar vesicles (LUVs) were prepared using a Mini-extruder (Avanti Polar Lipids) with 10 mm diameter drain discs and 100 nm diameter Nuclepore Track-Etched membranes (Whatman) passing the multilamellar membrane vesicles suspension 11 times through the filters at 25°C.

Leakage of vesicle aqueous contents

Melittin-induce release of aqueous vesicle content was measured by using the ANTS/DPX assay. PC, PC/PE/PS (50:40:10 w/w) or PC/PE/PS/PA (50:25:15:10 w/w) vesicles were prepared by extrusion of lipid suspension prepared in 50 mM Hepes buffer, pH 7, containing 30 mM NaCl, 12.5 mM of ANTS and 45 mM DPX as a quencher. Vesicles were separated from unencapsulated material on a Sephadex G-75 column (Sigma-Aldrich) by using 50 mM Hepes pH 7, containing 150 mM NaCl, as elution buffer. The final lipid concentration after exclusion chromatography was determined by phosphorus assay (Rouser et al. 1996). In a typical leakage assay, a given volume of melittin or melittin-PLGA-NP was added from a concentrated solution to the ANTS/DPX-loaded vesicles at 75 μM lipid. The resulting leakage was then followed by measuring the increase in fluorescence emission intensity at 536 nm, upon excitation at 353 nm, in a LS45 Perkin-Elmer spectrofluorometer. Complete (100%) release was achieved by the addition of 0.5% Triton X-100. All experiments were conducted at 25°C, and the apparent percentage of leakage was calculated according to the following equation:

$$\text{Leakage (\%)} = 100 \times (F - Fo)/(Ft - Fo)$$

where F and Ft represent the fluorescence intensity before and after the addition of detergent, respectively, and Fo represents the fluorescence of intact vesicles.

Results and Discussion

PLGA-NPs characterization

Melittin was encapsulated in PLGA-NPs by the water-in-oil-in-water ($W_1/O/W_2$) emulsion method optimized in our laboratory as previously described (Gonzalez et al. 2015). We characterized our PLGA-NP by undertaking the analysis of nanoparticle size and evaluating the amount of melittin adsorb in the PLGA-NP surface. DLS data indicated that nanoparticle size was 85 ± 20 nm ($n = 3$) with a narrow size distribution (Figure 1A) while the PDI < 0.1 confirmed that the particle was a typical monodisperse system. It is interesting to note that the incorporation of melittin in the PLGA-NPs leads to a narrow size distribution (Figure 1B) and to

an increase of nanoparticle size of 110 ± 20 nm (n = 3) as a result of adsorption of melittin at the nanoparticle surface.

Melittin basic amino acids (I^{20}-K^{21}-R^{22}-K^{23}-R^{24}-Q^{25}) are responsible for an electric interaction with the lutrol polar group present in nanoparticle, leading to a small increase in average particle size. Similar results had been observed by other authors using three kinds of polymers (Cui et al. 2005). It is well established that free melittin monomer is essentially a random coil molecule, whereas it displays a high α-helix content when it is bound to membranes (Vogel and Jähnig 1986). Once establish the amount of melittin incorporated into nanoparticle surface, CD spectroscopy was performed to evaluate the secondary structure of melittin in the PLGA-NPs.

Determination of melittin in PLGA-NPs

To characterize the properties of the peptide incorporated into nanoparticles it is necessary to precisely determine the protein content in nanoparticle suspension. Therefore, samples of nanoparticles (prepared as described in the Experimental section) were analyzed by two different methods: Bradford assay and direct determination of melittin incorporated in nanoparticles by analyzing the fluorescence intensity emitted by tryptophan 19 (excitation, 280 nm; emission, 351 nm) and interpolating the value on a calibration curve prepared for this purpose ($y = 49.036x + 1.17$; $R^2 = 0.9882$). As determined by the Bradford assay, the protein content in nanoparticle was 175 ± 2 μg and as determined by fluorescence intensity method, the amount of melittin incorporated was 170 ± 0.5 μg of the final nanoparticle suspension (average of three individual batches of nanoparticles). The percentage yield of melittin PLGA-NP was found to be 85%. Similar yields have been reported by Cui et al. (2005) for the preparation of PLGA-NPs by the double emulsion method. The mass ratio for vehicle: active was calculated and found that for every 40 mg of total solids (polymer and surfactant) is feasible to incorporate 170 μg of peptide. These values are consistent with those reported by other authors, which had evaluated the ability of interaction between PLGA particles and peptides or proteins and have shown a high interaction (Arroyo-Maya et al. 2014). However, it should be noted that the emission spectrum of melittin loaded PLGA-NP (Figure 2) appears to be blue-shifted (change in emission from 351 nm to 331 nm) and more intense when compared with the spectrum of melittin in solution; these differences in fluorescence properties are indicative of changes in the environment of aromatic residues that occur during the adsorption process. Specifically, the aforementioned spectral blue shift suggests that tryptophan (Trp) residue at position 19 is less exposed to the aqueous solvent in nanoparticle than native melittin. Similar results were observed for α-lactoalbumin when assembled into nanoparticles (Raghuraman et al. 2006). In the melittin tetramer, the intrinsic solvation probe of Trp is located at the junction between 2 α-helical monomers and is partially buried. However, Trp is fully exposed to the

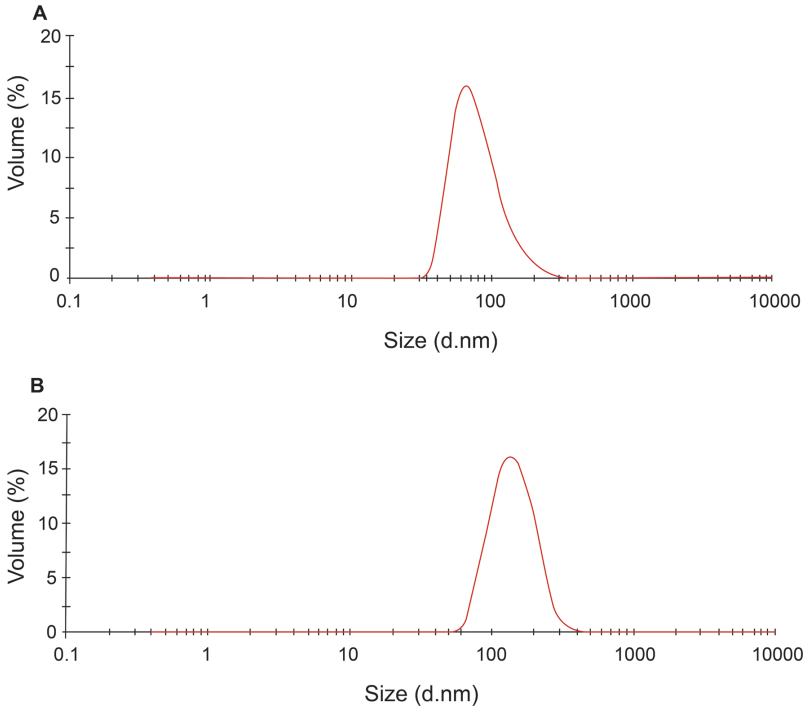

Figure 1. Mean size distribution of PLGA-NPs (**A**) and melittin-PLGA-NPs (**B**). The analysis was performed right after the preparation of the nanoparticle dispersions. The samples were diluted 50 times in Milli-Q water to reach a level of light scattering signal recommended by the supplier of the light scattering apparatus.

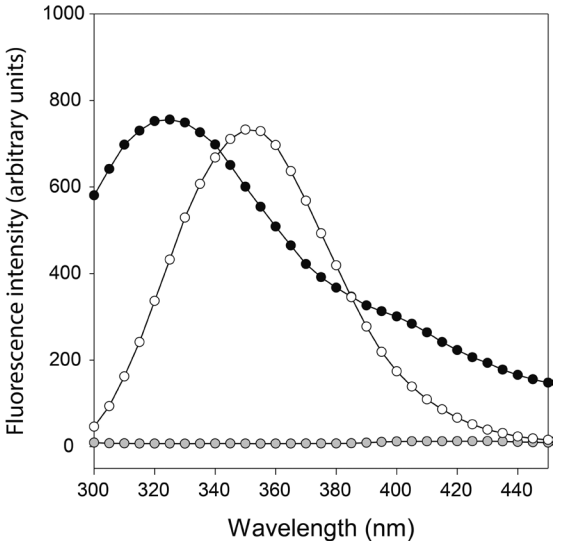

Figure 2. Fluorescence emission spectra of PLGA-NPs loaded with melittin. Intrinsic tryptophan fluorescence of melittin in solution (○), fluorescence of melittin-PLGA-NPs (●) and polymeric nanoparticles (●) are shown. The excitation wavelength (λ) was 280 nm and the final peptide concentration was 20 μg/ml.

solvent environment in the helical monomer. Raghuraman et al. reported that melittin tetramer is stabilized by increasing concentration of NaCl. The effect of NaCl on increasing the amount of tetramer starts around 0.25 M and the effect appears mainly for pH values less than 8 (Wilcox and Eisenberg 1992) so, at the conditions used in this work, the tetrameric structure was form before addition to nanoparticles, and remains stable after the addition to nanoparticle. To confirm this, it was monitored the α-helical content in PLGA-NP loaded with melittin by circular dichroism at 222 nm.

Conformational changes in melittin upon adsorption to nanoparticles

CD experiment (Figure 3) provides the idea about the secondary structure of monomeric and tetrameric melittin. Monomeric melittin shows a minimum at 205 nm, indicating the absence of any significant secondary structure in the peptide. The far UV spectrum of tetrameric melittin displays strength α-helical configuration with a broad negative band centered on 222 nm. It is well establish that increasing concentration of peptide and NaCl stabilizes melittin tetramer, so the stock solution prepared in this work agrees with these two conditions allowing melittin self-aggregation. Similar spectra were obtained by other authors in buffer 20 mM Tris, 150 mM NaCl (pH 7.4) at 25°C and peptide concentration of 0.5 mM (Goto and Hagihara 1992; Liao et al. 2015). By increasing peptide and NaCl concentration the conformation of melittin changes from a mainly random-coiled structure, with only 21% of α-helix, to a mainly helical one with 56%. Our observation is in line with the experimentally measured helicity obtained by other authors (Takahashi et al. 2013).

We compared the CD spectra of tetrameric melittin once incorporated in PLGA-NP to determine whether similar changes in the secondary structure of melittin occurred upon binding to the nanoparticles. Because control of PLGA-NP sample gave a flat ellipticity trace (see open circles in Figure 4), the CD band observed in melittin PLGA-NP can be attributed to the peptide present therein. The overall characteristics (i.e., peak position and ellipticity magnitude) of the spectrum clearly reflects the large number of a-helix regions found in this macromolecule, with double negative peaks at 222 nm and 208 nm and an helical content of 40%. Interestingly, the secondary structure of melittin PLGA-NP is similar to that reported as the CD spectra of tetrameric melittin at 0.5 mM peptide concentration, suggesting that tetramer formation remains stable after incorporation of peptide to nanoparticle. These results confirm that melittin interacts with the PLGA-NP and exists as a stably integrated component of the nanoparticle in its tetrameric form even in the absence of a monolayer membrane surrounding the nanoparticle. Using a hybrid melittin cytolytic peptide (Huang et al. 2013) and a different nanoparticle composition (Soman et al. 2008) other authors obtained similar results. We then assessed the functional activity of melittin bound to nanoparticles by determin-

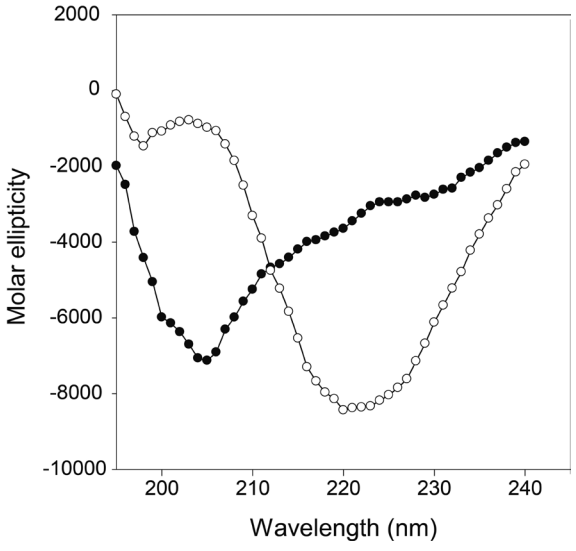

Figure 3. Circular dichroism (CD) spectra of monomeric (○) and tetrameric melittin (●). The peptide concentration used for the CD analysis was 70 μM. Data are reported as mean residue ellipticity. Monomeric and tetrameric melittin was prepared as described in Materials and Methods.

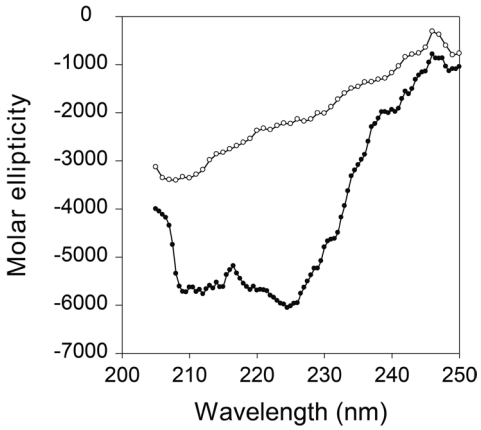

Figure 4. Circular dichroism spectra of free PLGA-NPs (○) and diluted suspension of tetrameric melittin-PLGA-NPs containing 100 μg of protein *per* milliliter (●). The samples were equilibrated in buffer Hepes 5mM pH 7.4. Data are reported as mean residue ellipticity.

ing pore formation upon interaction with liposomes that resembles breast cancer cell.

Kinetics of liposome leakage

Vesicles with different structures are used extensively in drug delivery and combinatory chemotherapeutic systems and can also be used to study artificial cell formation, which primitively mimics the membrane-based structure of eukaryotic cells (Paleos et al. 2012). Alterations of phospholipid profiles have been associated to disease and specific lipids may be involved in the onset and evolution of cancer. Doria et al. (2013) reported a lipidomic analysis of phospholipids from human mammary epithelial cells and breast cancer cell lines (MCF10A, T47-D and MDA-MB-231) using off-line thin layer chromatography (TLC) validated by hydrophilic interaction liquid chromatography-mass spectrometry. Differences in PE and PS content relative to total amount of phospholipids was highest in non-malignant cells while PA was present with highest relative abundant in metastatic cells (Doria et al. 2013). The phospholipids mixture used in this work for preparing liposomes where PC/PE/PS (50:40:10 w/w) to mimic membranes healthy mammary epithelial cells and the mixture PC/PE/PS/PA (50:25:15:10 w/w) to resemble the membranes of breast cancer cells. As representative compound of erythrocyte membrane, we used vesicles containing 100% PC. Membrane disruption by melittin PLGA-NP was characterized using a dye efflux assay. The assay is based on measuring the increase fluorescence that results from leakage of a quenched dye that is loaded into liposomes. The quenching property of fluorescence dye permits leakage from liposomes to be monitored continuously and is sensitive to small perturbation in the bilayer (Ralston et al. 1981). LUVs were filled with ANTS/DPX at concentration at which ANTS fluorescence is quenched by DPX. Upon leakage from the vesicle, quenching of the dye is relieved and a fluorescence signal is observed. PLGA-NP loaded with melittin induces leakage of the aqueous content

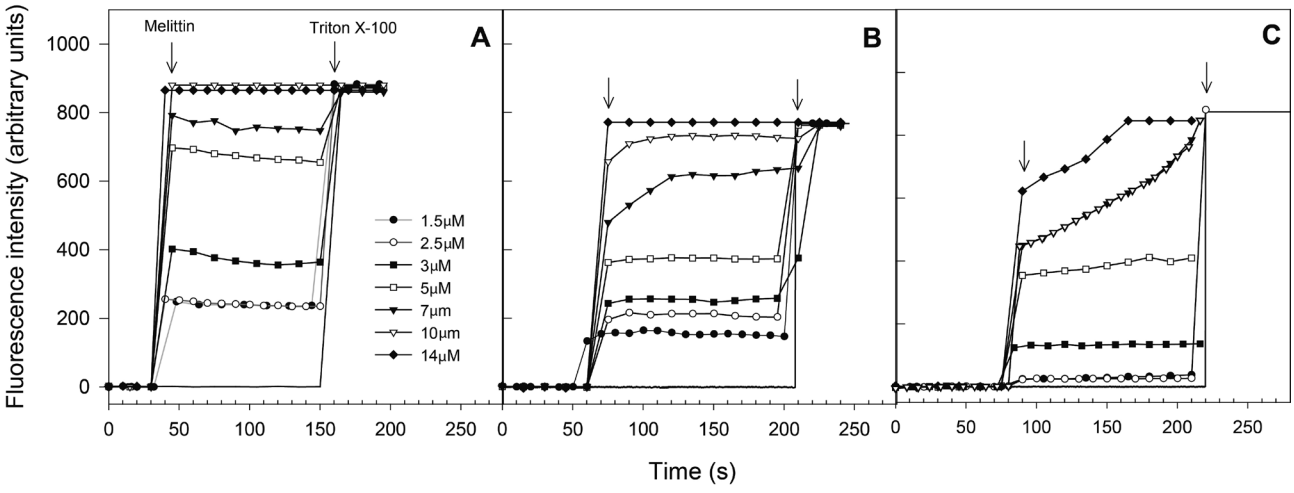

Figure 5. ANTS/DPX release induced by PLGA-nanoparticles loaded with melittin from PC/PE/PS/PA (50:25:15:10 w/w) vesicles (**A**); PC/PE/PS (50:40:10 w/w) liposomes (**B**) and PC vesicles (**C**). Peptide concentration assayed were 1.5, 2.5, 3, 5, 7, 10 and 14 μM. The final lipid concentration was 75 μM. Peptide-induced liberation of the fluorophores ANTS from the vesicles was followed by monitoring fluorescence emission using excitation and emission wavelengths of 353 and 536 nm, respectively. The percentage of leakage induced by any given peptide concentration was estimated taking as a reference the maximum possible leakage, obtained after addition to the samples of an aliquot of Triton X-100 (final concentration of 0.5%, v/v).

from each kind of LUVs tested. The effect of phospholipid composition on the lytic power of melittin-PLGA-NP is shown in Figure 5. Initially, no fluorescence is observed in all cases since the high concentration (45 mM) of DPX used resulted in quenching of ANTS fluorescence. Upon addition of melittin-PLGA-NP, the entrapped ANTS/DPX were released into the buffer due to membrane perturbation, leading to the dilution of the DPX quenching effect, increasing ANTS fluorescence. The extent of increase in fluorescence intensity is a measure of the lytic power of melittin in a given membrane environment. As is evident from the figure the lytic efficiency of nanoparticle-melittin in different vesicles is clearly dependent on the composition of the membrane: slightly higher lytic activity is observed in the presence of PA at any peptide concentration an also, the membrane perturbation effect occurs immediately after being added the peptide (Figure 5A). In the case of liposomes that resembles healthy mammary epithelial cells (PC/PE/PS 50:40:10 w/w) it can be observed that with the last three peptide concentrations evaluated, achieve the maximum lytic activity takes a few seconds before fluorescence intensity reaches a plateau indicating that no further release occurs after a certain period (Figure 5B). For liposomes that resemble erythrocyte membrane (PC vesicles), the natural target of melittin, the kinetics also show that achieve the maximum lytic activity takes a few seconds before fluorescence intensity reaches a plateau. It can be observed how from 10 μM peptide concentration takes longer to disrupt the lipid bilayer (Figure 5C). In all liposomes used in this work, the time required for melittin-PLGA-NP to produce maximum leakage, as well as the maximal amount o fluorescence liberated were both dependent on peptide concentration.

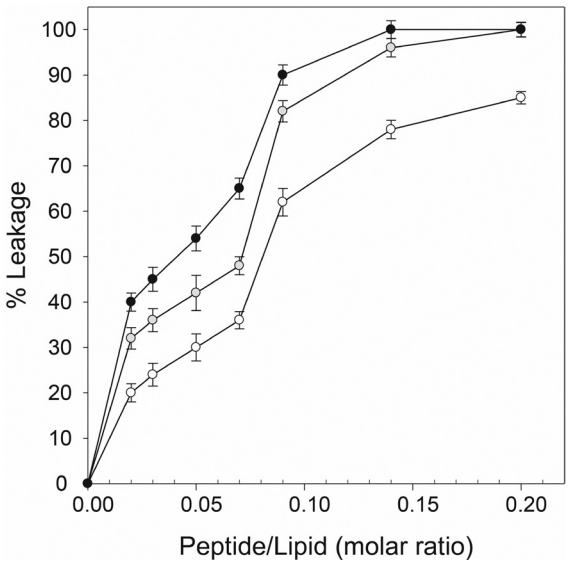

Figure 6. Effect of melittin-PLGA-NPs on the leakage from PC (○), PC/PE/PS (50:40:10 p/p) (●) and PC/PE/PS/PA (50:25:15:10 w/w) (●) large unilamellar vesicles. Peptide concentration assay were 0.6, 0.8, 1.2, 1.8, 2.4, 3.6, 4.8 μM and the final lipid concentration was 25 μM. Peptide-induced liberation of the fluorophore ANTS from the vesicles was followed by monitoring fluorescence emission using excitation and emission wavelengths of 353 nm and 536 nm, respectively. The percentage of leakage induced by any given peptide concentration was estimated taking as a reference the maximum possible leakage obtained after addition to the samples of an aliquot of Triton X-100 (final concentration 0.5% v/v). The typical error from at least two independent experiment is indicated.

The lipid disruption properties of melittin-PLGA-NP are summarized in Figure 6; it can be observed how the incorporation of melittin to PLGA-NP do not alter the cytolytic ability of this peptide on any of the phospholipid vesicles analyzed. Melittin-PLGA-NP were able to disrupt 50% of the PC LUVs at concentrations of around 2 μM. The nanoparticles loaded with tetrameric melittin were more effective inducing leakage from PC/PE/PS (50:40:10 w/w) and PC/PE/PS/PA (50:25:15:10 w/w) at around 1.2 μM and 1.8 μM, respectively.

It has been reported that under similar experimental conditions, free melittin originate leakage from zwitterionic liposomes at around 0.25 μM and at 0.4 μM from liposomes containing 10% molar of negatively charged phospholipids (Higashino et al. 2001; Van den Bogaart et al. 2008; Soman et al. 2009) which represents an increase of about 8% in peptide concentration comparing with our results for zwitterionic liposomes and an increase of 3% for liposomes containing PS and 5% of liposomes with PA; so the tetrameric conformation of melittin incorporated in PLGA-NPs form a hydrophobic patch when a helical region is structured, reducing the lytic activity from zwitterionic lipids while retains its cytotoxic activity against anionic membranes. These results are in accordance with observations made by Pandey et al. (2010) who reported increasing cell selectivity using a Leu9Ala mutation which exhibited significantly reduce hemolytic activity than that of native melittin, while the analogues of melittin showed comparable antibacterial activities to melittin against Gram-positive and -negative bacteria (Pandey et al. 2010).

It is important to note that the lytic activity of our tetrameric melittin-PLGA-NP is more cytotoxic than other melittin-nanoparticle system reported. Huang et al. (2013) designed a hybrid cytolytic peptide, α-melittin in which the N-terminus of melittin is linked to the C-terminus of an amphipathic α-helical peptide *via* a GSG linker. These α-melittin-nanoparticles induced minimal hemoglobin release at concentration of 50 μM while the cytotoxicity in tumor cells was reached at 11.26 μM. This represents a tolerance of about 10 times more than our system for PC membranes

and around 2 times more for membranes containing anionic phospholipids. Soman et al. (2009) observed a more protective action against red blood cell hemolysis with the use of lipid-based melittin-perfluorocarbon nanoparticles; they report that even a concentration of 25 μM nanoparticle-melittin only elicited 10% hemolysis. So it is clear that to reduce melittin hemolytic activity is necessary to shield its hydrophobic N-terminal segment either through structural changes or alteration in melittin sequence or by conjugation with other hydrophobic molecules. In this light, our results demonstrated that is therefore possible to selectively favor melittin aggregation and preserve the complex peptide structure in an active form once incorporated to PLGA-NP. However, we need to improve our formulation system to reduce even more melittin lytic activity on membrane model systems that aims to conduct hemolytic assays using red blood cells.

Conclusion

To summarize, our goal in this study was to formulate stable high payload PLGA particles as nanovehicles for tetrameric melittin and evaluate its utility as a cancer chemotherapeutic agent in a model bilayer membrane system. Our results indicate that melittin tetrameric conformation in PLGA-NP is able to slightly reduce the lytic activity of this peptide over mammalian cell membrane mimetic model membranes, supporting a crucial role for hydrophobic region to permeabilize zwitterionic liposomes, although the reduction observed it is not enough for *in vivo* administration. It is to be mentioned that our nanoparticle-system induced significant and very similar leakage in the PC/PE/PS and PC/PE/PS/PA lipid vesicles, which indicate that tetrameric melittin conformation retain the ability to permeabilize the negatively charged lipid membranes. Additional research is needed to investigate the mechanisms by which tetrameric melittin-PLGA-NP interact and perturb lipid bilayers. We need to improve our nanoparticle formulation to reduce even more melittin lytic activity that aims to conduct hemolytic assays using red blood cells and also cell viability assays against endothelial and breast cancer cell lines to translate our findings into useful therapeutic potential.

Acknowledgments. This research was financially supported by the Consejo Nacional de Ciencia y Tecnología (CONACYT), Project No. C.B. 2014 236834.

Conflicts of interest. None declared.

Author contributions. Conceived and designed the experiments: A.G.H., A.Ch.M.; performed nanoparticle preparation and leakage experiments: A.M.A.; performed CD experiments: A.G.H.; analyzed the data and wrote the paper: A.G.H. The authors are thankful to Jessica Paola Mendez Chavero for her experimental support in nanoparticle preparation. All authors read and approved the final manuscript.

References

Allende D., Simon S. A., McIntosh T. J. (2005): Melittin-induced bilayer leakage depends on lipid material properties: evidence for toroidal pores. Biophys J. **88,** 1828–1837 https://doi.org/10.1529/biophysj.104.049817

Arroyo-Maya I. J., Hernandez-Sanchez H., Jimenez-Cruz E., Camarillo-Cadena M., Hernandez-Arana A. (2014): a-Lactoalbumin nanoparticles prepared by desolvation and cross-linking: Structure and stability of the assembled protein. Biophys. Chem. 193-194, 27–34 https://doi.org/10.1016/j.bpc.2014.07.003

Bala I., Hariharan S., Kumar M. N. (2004): PLGA nanoparticles in drug delivery: The sate of the art. Crit. Rev. Ther. Drug Carrier Syst. **21,** 387–422 https://doi.org/10.1615/CritRevTherDrugCarrierSyst.v21.i5.20

Cui F., Cun D., Tao A., Yang M., Shi K., Zhao M., Guan Y. (2005): Preparation and characterization of melittin-loaded poly (DL-lactic acid) or poly (DL-lactic-co-glycolic acid) microspheres made by the double emulsion method. J. Con. Rel. **107,** 310–319 https://doi.org/10.1016/j.jconrel.2005.07.001

Doria M. L., Cotrim C. Z., Simoes C., Macedo P. D., Dominguez R., Helguero L. A. (2013): Lipidomic analysis of phospholipids from human mammary epithelial and breast cancer cell line. J. Cell. Physiol. **228,** 457–468 https://doi.org/10.1002/jcp.24152

Gajski G., Cimbora-Zovko T., Osmak M., Garaj-Vrhovac V. (2011): Bee venom and melittin are cytotoxic against different types of tumor and non-tumor cell lines in vitro. Cancer Res. J. **4,** 159–174

Gonzalez E., Gonzalez A., Castro R., Luna H., Chavez A. (2015): Implementacion de la tecnica de doble emulsion para la microencapsulacion polimerica de moleculas ionicas. Rev. Ib. Ci., **2,** 117–125

Goto Y., Hagihara Y. (1992): Mechanism of the conformational transition of melittin. Biochemistry **31,** 632–738 https://doi.org/10.1021/bi00118a014

Habermann E. (1977): Bee and wasp venoms. Science **177,** 314322

Higashino Y., Matsui A., Ohki K. (2001): Membrane fusion between liposomes composed of acidic phospholipids and neutral phospholipids induced by melittin: A differential scanning calorimetric study. J. Biochem. **130,** 393–397 https://doi.org/10.1093/oxfordjournals.jbchem.a002998

Huang C., Jin H., Qian Y, Qi S., Luo H., Luo Q., Zhang Z. (2013): Hybrid melittin cytolytic peptide-driven ultrasmall lipid nanoparticles block melanoma growth in vivo. ACS Nano **7,** 5791–5800 https://doi.org/10.1021/nn400683s

Jamasbi E., Batinovic S., Sharples R., Sani M. A., Robins-Bowne R. M., Wade J. D., Sparovic F., Hossain M. A. (2014): Melittin peptides exhibit different activity on different cells and model membranes. Amino Acids **46,** 2759–2766

https://doi.org/10.1007/s00726-014-1833-9
Jeong Y. J., Choi Y., Shin J. M., Cho H. K., Kang J. H., Park K. K., Choe J. Y., Chang Y. C. (2014): Melittin suppresses EFG-induced cell motility and invasion by inhibiting PI3K/Akt/mTOR signaling pathway in breast cancer cells. Food Chem. Toxicol. **68,** 218–225
https://doi.org/10.1016/j.fct.2014.03.022
Liao C., Myvizhi E., Zhao J., Slimovitch J., Schneebeli S., Shelley M., Shelley J., Li J. (2015): Melittin aggregation in aqueous solutions: insight form molecular dynamics simulation. J. Phys. Chem. B **119,** 10390–10398
https://doi.org/10.1021/acs.jpcb.5b03254
Liu S., Yu M., He Y., Xiao L., Wang F., Song C., Ling C., Xu Z. (2008): Melittin prevents liver cancer cell metastasis through inhibition of the Rac1-dependent pathway. Hepathology **47,** 1964–1973
https://doi.org/10.1002/hep.22240
Paleos C. M., Tsiorvas D., Sideratou Z. (2012): Preparation of multi-compartment lipid-based systems based on vesicle interactions. Langmuir **28,** 2337–2346
https://doi.org/10.1021/la2027187
Pan H., Soman N. R., Sclesringer P. H., Lanza G. M., Wickline S. A. (2011): Cytolytic peptide nanoparticles (NanoBees) for cancer therapy. Wiley Interdiscip. Rev. Nanomed. Nanobiotechnol. **3,** 318–327
https://doi.org/10.1002/wnan.126
Pandey B. K., Ahmad A., Asthana N., Azmi S., Srivastava R. M., Srivastava S.,Verma R., Vishwakarma A. L., Ghosh J. K. (2010): Cell-Selective lysis by novel analogues of melittin against human red blood cells and Escherichia coli. Biochemistry **49,** 7920–7929
https://doi.org/10.1021/bi100729m
Park M., Kim J., Jeon J., Park J., Lee B. J., Suh G. H., Cho Ch. W. (2015): Preformulation studies of bee venom for the preparation of bee venom-loaded PLGA particles. Molecules **20,** 15072–15083 DOI:10.3390/molecules200815072
https://doi.org/10.3390/molecules200815072
Pott T., Maillet J. C., Abad C., Campos A., Dufourcq J., Dufourc E. J. (2001): The lipid charge density at the bilayer surface modulates the effects of melittin on membranes. Chem. Phys. Lipids **109,** 209–223
https://doi.org/10.1016/S0009-3084(00)00223-1
Raghuraman H., Chattopadhyay A. (2004a): Effect of micellar charge on the conformation and dynamic of melittin. Eur. Biophys. J. **33,** 611–622
https://doi.org/10.1007/s00249-004-0402-7
Raghuraman H., Chattopadhyay A. (2004b): Influence of lipid chain unsaturation on membrane-bound melittin: a fluorescence approach. Biochem. Biophys. Acta **1665,** 29–39
https://doi.org/10.1016/j.bbamem.2004.06.008
Raghuraman H., Ganguly S., Chattopadhyay A. (2006): Effect of ionic strength on the organization and dynamics and membrane-bound melittin. Biophys. Chem. **124,** 115–124
https://doi.org/10.1016/j.bpc.2006.06.011
Raghuraman H., Chattopadhyay A. (2007): Melittin: a membrane-active peptide with diverse functions. Biosci. Rep. **27,** 189–223
https://doi.org/10.1007/s10540-006-9030-z
Ralston E., Hjelmeland H. M., Klausner R. D., Winstein J. N., Blumenthal R. (1981): Carboxyfluorescein as a probe for liposome-cell interactions. Effect of impurities, and purification of the dye. Biochem. Biophys. Acta **649,** 133–137
https://doi.org/10.1016/0005-2736(81)90019-5
Rouser G., Siakotos A. N., Fleischer A. S. (1996): Quantitative analysis of phospholipids by thin-layer chromatography and phosphorus analysis of spots. Lipids **1,** 85–86
https://doi.org/10.1007/BF02668129
Scholtz J., Qian H., York E. J., Stewart J. M., Baldwin R. L. (1991): Parameters of helix-coil transition theory for alanine-based peptides of varying chain lengths in water. Biopolymers **31,** 1463–1470
https://doi.org/10.1002/bip.360311304
Shigeri Y., Horie M., Yoshida T., Hagihara Y., Imura T., Inagaki H., Haramoto Y., Ito Y., Asashima M. (2016): Physicochemical and biological characterizations of Pxt peptides from amphibian (Xenopus tropicalis) skin. J. Biochem. **159,** 619-629
https://doi.org/10.1093/jb/mvw003
Soman N. R., Lanza G. M., Heuser J. M., Schlesinger P. H., Wickline S. A. (2008): Synthesis and Rcharacterization of stable fluorocarbon nanostructures as drug delivery vehicles for cytolytic peptides. Nano Letters **8,** 1131–1136
https://doi.org/10.1021/nl073290r
Soman R. N., Baldwin S. L., Hu G., Marsh J. N., Lanza G. M., Heuser J. E., Arbeit J. M., Wickline S. A., Schlesinger P. H. (2009): Molecularly targeted nanocarriers deliver the cytolytic peptide melittin specifically to tumor cells in mice, reducing tumor growth. J. Clin. Invest. **119,** 2830–2842
https://doi.org/10.1172/JCI38842
Takahashi T., Nomura F., Yokoyama Y., Tanaka-Takaguchi Y., Homma M., Takaguchi K. (2013): Multiple membrane interactions and versatile vesicle deformations elicited by melittin. Toxins **5,** 637–664
https://doi.org/10.3390/toxins5040637
Van den Bogaart G., Velasquez Guzman J., Mika J. T., Poolman B. (2008): On the mechanism of pore formation by melittin. J. Biol. Chem. **49,** 33854–33857
https://doi.org/10.1074/jbc.M805171200
Vogel H., Jähnig F. (1986): The structure of melittin in membranes. Biophys. J. **50,** 573–582
https://doi.org/10.1016/S0006-3495(86)83497-X
Wilcox W., Eisenberg D. (1992): Thermodynamics of melittin tetramerization determined by circular dichroism and implications for protein folding. Protein Science **1,** 641–653
https://doi.org/10.1002/pro.5560010510
Yang D., Harroun T. A., Weiss T. M., Ding L., Huang H. W. (2001): Barrel-stave model or toroidal model? A case study on melittin pores. Biophys. J. **81,** 1475–1485
https://doi.org/10.1016/S0006-3495(01)75802-X

Received: October 21, 2016
Final version accepted: March 6, 2017
First published online: June 27, 2017